Desalination and Water Treatment
www.deswater.com

doi: 10.5004/dwt.2019.23335

138 (2019) 219–229
January

Disposal of cesium ion from wastewater using biocompatible titanate nanotube

Sayed Mustafa Banihashemi Jozdani[a,b,*], Abdolreza Nilchi[c,*], Shahrzad Abdolmohammadi[a]

[a]*Department of Chemistry, East Tehran Branch, Islamic Azad University, P.O. Box 18735-138, Tehran, Iran, emails: Banihashemi313@yahoo.com (S.M. Banihashemi Jozdani), abdolmohamadi_sh@yahoo.com (S. Abdolmohammadi)*
[b]*Department of Cell Engineering, Cell Science Research Center, Royan Institute for Stem Cell Biology and Technology, ACECR, Tehran, Iran*
[c]*Materials and Nuclear Fuel Research School, Nuclear Science and Technology Research Institute, P.O. Box 11365-8486, Tehran, Iran, email: anilchi@aeoi.org.ir*

Received 7 April 2018; Accepted 23 October 2018

ABSTRACT

Due to the extensive use of radioisotopes, effective methods to manage radioactive waste are highly required. For this reason, the capture of cesium ion from groundwater and aquatic ecosystems has attracted special attention. In the present study, the synthesized titanate nanotubes can be applied to remove cesium ion from aqueous solutions through the cation exchange process. In addition, the ion exchange properties of titanate nanotubes were investigated by calculation of the adsorption of cesium ion through the batch method. Hence, the effect of initial concentration, pH and the contact time of solution and exchanger phases on the adsorption value and the optimum conditions for optimal performance of exchanger for the capture of cesium ion were determined. In this regard, the titanate nanotube was synthesized hydrothermally at the optimum temperature of 150°C. After that, 0.1 g of this titanate nanotube was exposed to 50 mg/L of cesium ion at pH = 6 and 25°C temperature in 25 mL of wastewater. Batch experiments confirmed that around 85% of cesium ion (4.25 mg/mL) could be captured 90 min after induction. In addition, in order to evaluate the biocompatibility of these titanate nanotubes, MTT assay was used for their cytotoxicity potential. X-ray diffractometer analysis represented a nanoscale composition with anatase phase which showed that the arranged titanate nanotube was crystallized and had a BET surface area of 194.4 m^2/g. Furthermore, the kinetic data were described with pseudo-first and second-order models, and results showed that the Freundlich model was more suitable than the Langmuir model to describe the equilibrium of cesium ion.

Keywords: Aquatic pollution; Cesium adsorption; Titanate nanotube; Hydrothermal method

1. Introduction

The growth of the human population besides the development of industrial processes leads to increase of the production, consumption, and disposal of chemicals and contaminants as waste. The ultimate receiver of this increasing range of anthropogenic wastes is the aquatic system. This issue plays a vital role in ecosystem preservation, human health, and civilization. In addition, there is an increasing public demand for clean water, and there are concerns over the presence of a variety of anthropogenic contaminants in the aquatic environment [1]. For example, effluent water can be contaminated mostly with so many organic dyes which are hardly bio-degradable. Furthermore, around 1.4 million km^2 of the lands in China were covered by a hazardous dense material in January 2013, which lead to the death of more than 800 million people. This issue leads to evaluate the removal of these chemicals because of their potentially genotoxic and carcinogenic influences [2].

* Corresponding authors.

1944-3994/1944-3986 © 2019 Desalination Publications. All rights reserved.

Cesium-137 ($^{137}Cs^{+}$) with the half-life of 30 years is a strong toxic radioactive pollutant produced through fission of uranium-235 (^{235}U). This radionuclide emits radioactivity for decays, in the form of beta particles and relatively strong gamma radiation. Cesium salts, the most well-known form of the element, which is easily dissolved in the water, causes serious concerns about exposure levels of a possible accident that may happen in a nuclear reactor; such as those that occurred at Three Mile Island in Pennsylvania in 1979, Chernobyl in 1986 and the last one in 2011 at Fukushima, Japan [3–6].

The data received from several years of observations about the leak of radioactive $^{137}Cs^{+}$ at Chernobyl accident and nuclear power stations in Britain, Germany, and the United States, represented that radioactive $^{137}Cs^{+}$ are accumulated in mushrooms [7], mosses [8], lichens [9], and even in plants such as grasses, ferns, heathers, and blueberries [10]. Finally, these organisms can be directly or indirectly entered into the food chain and transferred to other living organisms, including humans [5]. These findings have raised concerns about the exposure of communities living around it and causing serious threats for present and next generations [6,11]. In this regard, because of the extensive use of radioisotopes and nuclear power, effective methods to manage radioactive wastes are required, this is a critical part of the nuclear energy process [12].

There are many practical approaches and technologies developed for disposal and removal of radioactive aqueous wastes which are produced at different stages of a nuclear disaster. Some of these technologies, including co-precipitation with ferrocyanides [13], ammonium molybdophosphates [14], macrocyclic ethers [15], solvent extraction with dicarbollylcobaltate (III) [16], and ion exchange sorbents [5].

Most of the existing methods are so complicated and expensive [17]. Therefore, finding an inexpensive, effective, specific, and high-efficiency cesium ion adsorbent from groundwater and aquatic ecosystems has attracted scientist's attention [18].

To separate $^{137}Cs^{+}$ ions from nuclear waste, many inorganic ion exchange sorbents, such as crystalline silicotitanate, zeolite, clay minerals, layered zirconium phosphate, and sulphide layers, have been studied so far [6,19,20].

Titanate is the salt of the polytitanic acid which [21] has constant chemical, thermal, and mechanical features over the time [22]. It has been proven that titanate shows great potential for applications in adsorption, lithium ion batteries, biomedical studies, and oil–water separation, due to its physical–chemical properties and particular crystalline structure [2]. TiO_6 octahedral, a layered structure, is the basic structural unit for titanate nanostructures [23,24]. Layered titanate material represents some attractive features including high and fast ion-exchange capacity, and high surface charge density [25]. Another feature of titanate which attracts much more attention is its ability to transform into titanium dioxide (TiO_2). This capability allows the use of titanate as flexible precursors of TiO_2 nanostructure [2]. Considering the crystallinity, morphology, size, content, and surface characteristics, nanostructures of titanate can be synthesized in various forms, including titanate nanotubes (TNTs) and nanowires are the two most popular representatives of the titanate nanomaterial family [21].

Due to their unique ion-exchange properties, titanate nanostructures represent a high tendency for binding to inorganic cations including radionuclide. Different studies reported that TNTs can be easily fabricated at low cost using a hydrothermal method [22,26,27].

The ion exchange process is often irreversible when the structure collapses upon ion exchange with most of the bivalent and trivalent cations (e.g., Hg^{2+}, Pb^{2+}, Cr^{3+}) [21]. But, when the diameter of the metal ion is small enough (e.g., $^{137}Cs^{+}$) to be inserted into the layered spaces of titanate nanostructures, the reversible ion-exchange process is mainly accrued [2]. Layered nanotitanates immobilize the targeted $^{137}Cs^{+}$ ions using Na^{+} ions situated using reversible interactions. Technically, these nanostructures provide a high surface area, which offers a high and fast capacity to adsorb radioisotopes [22,28]. The adsorption of $^{137}Cs^{+}$ ion during the reversible process provides the possibility of accessing the deposits of adsorbents from water resources, and then there will be the opportunity to extract $^{137}Cs^{+}$ ion from the TNTs during the refractory process and use them for further adsorption.

There are several studies showing the widespread use of TNTs in drug delivery [26], industrial products [29], toothpaste, cosmetics, paints, paper, plastic, and food products [30]. In this research, we tried to synthetize TNTs to capture $^{137}Cs^{+}$ ions from aqueous solution. The increasing application of TNT brings up a serious concern about the investigation of its toxicity. For this reason, the distinct amount of synthesized TNT was analyzed for their cytotoxicity effects.

The main purpose of this study was to investigate the conditions in which TNTs can be applied to remove $^{137}Cs^{+}$ ions from the aqueous environment (i.e., pH, time of exposure, sorbent mass, cesium mass, and temperature) through cation exchange process. But, in addition to the main purpose, it was important for us to improve a method to synthesize these nanotubes in order to introduce a biocompatible nanoparticle in the biological ecosystem.

2. Experimental setup

2.1. Material and instruments

The chemical materials and reagents utilized in this study were of analytical grade which is including NaOH (Merck, United States), HCl (Merck, United States), HNO_3 (Merck, United States), TiO_2 (Merck, United States), $CsNO_3$ (Merck, United States), $^{137}Cs^{+}$ (Pars Isotope, Iran), and $[Si(CH_3)_2O–]_n$ (Sigma-Aldrich, United States). To identify the synthesized TNT, crystal structures, amount and type of elements, specific surface area, average pore diameters, and cytotoxicity effect of these synthesized nanotubes, the following instruments were used subsequently; transmission electron microscopy (TEM) (CM20, 200 kV, Philips, Germany), field emission scanning electron microscopy (FESEM) (MIRA3TESCAN-XMU), infrared spectroscopy (FTIR) (Vector22, Bruker, United States), X-ray diffractometer (XRD) (Philips PW 1130/90), and absorbance microplate reader (ELX800, BioTek, United States). The concentration of the elements (absorption rate) was measured using atomic absorption spectrophotometer (AAS) (model 843, FRG, PerkinElmer, United States). The pH adjustments were carried out using pH meter (model 827, Metrohm, Switzerland) and agitation of the solution was applied by centrifuge instrument (J-21C, Beckman, United States).

2.2. Preparation of TNT adsorbent

In this study, TNTs were synthesized hydrothermally, similar to Zhu et al. [22] basic protocol but with some modifications. In this regards, 180 mL sodium hydroxide (NaOH) 10 M solution and 7.0 g TiO_2 powder were mixed using a magnetic stirrer in a Teflon container. After that, the feedstock solution was first autoclaved in an oil bath for 2 h and subsequently kept in the oven for 72 h at 150°C to complete the synthesis process. The product was then cooled slowly at room temperature, washed several times with 0.1 M hydrochloric acid and distilled water until reached pH = 6–7, and centrifuged at 600 × g for 15 min. The supernatant discarded and the sediment was dried in the oven at 300°C for 3 h to form the desired adsorbent powder. To access much more homogenized powder, the precipitate was passed thorough standard sieve containing 220-μm pore size.

2.3. Characterization of TNT adsorbent

Phase identification and crystallite size of the TNT adsorbent were determined by XRD analysis using a scan speed of 2°/min and Cu Kα (λ = 0.154056 nm) radiation source. Formation and microstructure of TNTs were further confirmed by FTIR (spectral region 400–4,000 cm), FESEM (50, 20, 10, and 5 μm) and TEM (200, 100, 60 nm size). Brunauer–Emmett–Teller (BET) analysis measured the specific surface area and Barrett–Joyner–Halenda (BJH) method calculated pore size distribution through nitrogen adsorption/desorption isotherms.

2.4. Cytotoxicity effect of titanate nanotube

Fibroblast cells derived from human gingival (HUGU) were used for investigation of the cytotoxicity effect of TNT (IBRC, Iran). HUGU cells were appropriate candidate for cytotoxicity investigations because of the human digestive system can be the final receiver of harmful ions from the food chain. In this regards, HUGU cells were cultured in Dulbecco's modified eagle medium containing 10% FBS and 2 mM L-glutamine at 37°C with 95% humidity and 5% CO_2. After the cells grow and reach to appropriate numbers, 1.5×10^4 HUGU cells were seeded in each 96-well plates, and then cells were exposed to distinct concentrations of TNT (0.01, 0.02, 0.04, 0.08, 0.1, 0.2, 0.4, 0.8, 1, and 10 mg/mL) for 24 h. MTT method was applied to study the TNT influence on cell viability [31]. For this reason, formazan dye absorbance was measured at 570 nm (and 630 nm used as a reference wavelength) with an absorbance microplate reader. Cell viability was expressed based on the untreated control group (negative control).

2.5. Batch experiments

2.5.1. Investigation of TNT concentration on adsorption

For investigation of TNT performance, 0.01–0.25 g of TNT was added to 25 mL of cesium solution (50 mg/L) and the sample was then placed in a thermostatic shaker (25°C) for 90 min after the time interval, the supernatant solutions were filtered and the concentration of cesium was determined by atomic absorption spectroscopy (AAS), and then the absorption efficiency was calculated.

2.5.2. Effect of time on cesium absorption

The effect of time for adsorption of cesium ion using TNT was analyzed in the range of 10–180 min. For this reason, the optimum titanate concentration (0.1 g) was added to 25 mL of cesium solution (50 mg/L). After homogenization using thermostatic shaker, the absorption efficiency was obtained at the times of 10, 20, 35, 60, 120, and 180 min after exposure. This process was calculated using AAS technique.

2.5.3. Effects of pH and agitator type on cesium adsorption

In order to evaluate the effect of pH on the adsorption rate, 25 mL of cesium ion (50 mg/L) was mixed with 0.1 g of TNT at 25°C for 90 min. This solution was performed in the several test tubes and then exposed to different acidic conditions (pH = 2–7). For each experimental condition, AAS analysis was evaluated.

In addition, for investigation of the effect of agitator type, either magnetic stirrer or mechanical shaking, the solution containing 25 mL of cesium ion (50 mg/L) was mixed with 0.1 g of TNT at 25°C for 90 min. This solution agitated using different types of stirrer mentioned above. Subsequently, the adsorption rate of each experimental condition was determined using AAS.

2.5.4. Effect of temperature on cesium adsorption

In order to analyze the effect of different temperatures on the adsorption rate, 0.1 g of TNT was added to 25 mL of cesium solution (50 mg/L). This solution was homogenized using a thermostatic shaker for 90 min, in a temperature range of 10°C–75°C. The cesium adsorption rates were then calculated at different temperature using AAS.

2.5.5. Effect of cesium equilibrium concentration

After adjustment of the pH to the expected range (pH ≈ 6), cesium ion was aliquot in several high-density 25 mL polypropylene bottles (in the different concentration containing 10–120 mg/L). Then, 0.1 g of TNT adsorbent was added to each of these test solutions, and the samples were then placed in a thermostatic shaker for homogenization during 90 min. The solutions were then used to determine the concentration of cesium ion by AAS.

Furthermore, for isotherm studies, the concentration of cesium ion which retained in the titanate nanotube adsorbent (mg/g), was calculated by Eq. (1):

$$q_e = (C_0 - C_e) \times \frac{V}{M} \tag{1}$$

According to this formula, V is the aqueous solutions volume (mL), M is the sorbent weight (g), and C_0 and C_e are the initial and final ion(s) concentrations (mg/L), respectively.

In order to identify the nature of adsorption, the experimental data were analyzed with the Freundlich and Langmuir formula.

3. Results and discussion

3.1. Titanate nanotube physicochemical characterization

Several methods including FTIR, TEM, FESEM, XRD, and BET were applied for characterization and confirmation of the synthesized TNTs in this study.

3.1.1. FTIR spectrum

Fig. 1 represents the FTIR spectrum at 400–4,000 cm^{-1} for TNT synthesized by hydrothermal method. The presence of a peak at 450–700 cm^{-1} indicates the Ti–O and Ti–O–Ti bond which corresponding to skeletal frequency regions. Also, finding the peak at 1,600 cm^{-1} indicates the bending vibration of HOH and a peak at 3,400 cm^{-1} indicate the tensile vibration of hydroxyl groups (OH) that confirms the presence of water and also hydroxyl groups in the nanotube structure. The peak within the range of 900 cm^{-1} indicates the one-dimensional structure of the nanotube titanate.

3.1.2. XRD analysis

The XRD pattern of nanotube titanate powder is shown in Fig. 2. The shortness and expansion of the pixels after TNT synthesis in hydrothermal conditions (Fig. 2(b)) indicate a change in the morphology of the TiO_2 structural pattern (Fig. 2(a)) which leads them to a nanoscale composition.

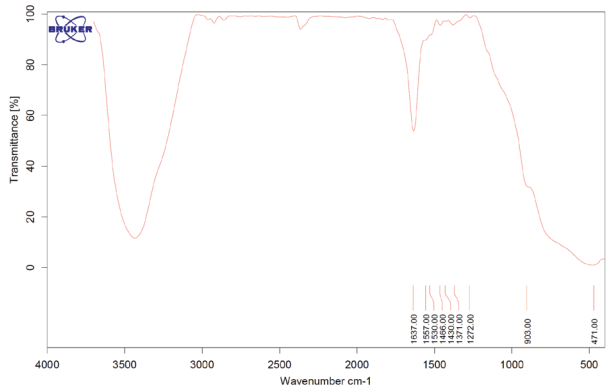

Fig. 1. FTIR spectra of the titanate nanotube.

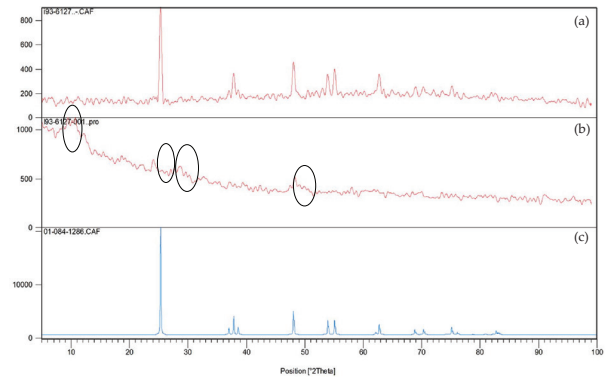

Fig. 2. XRD pattern for (a) TiO_2 powder, (b) titanate nanotube, and (c) TiO_2 derived from high score software as a standard.

Experimental analysis represented that both anatase and rutile structures are visible in the component. XRD data showed score 77 for TNT anatase phase and score 10 for rutile phase, which confirmed TiO_2 chemical formula. Titanate nanotube represented the anatase phase in three identified peaks (2θ: 24°, 28°, and 48°) which confirms a structure such as $A_2Ti_2O_5{\cdot}H_2$ and $A_2Ti_3O_7$. In addition, at 2θ ~ 9.5° a weak slope was observed which seems to be related to the distance between the TNTs wall layer [32]. The structures of $Na_2Ti_2O_4(OH)_2$ or $H_2Ti_2O_4(OH)_2$ are most probable for TNT in which Na^+ ion has been replaced by H^+ ion during ion exchange process. This structure can also be presented as $Na_2Ti_2O_5{\cdot}H_2O$ and $H_2Ti_2O_5{\cdot}H_2O$ [33,34].

3.1.3. FESEM and TEM investigation

FESEM and TEM results in Figs. 3 and 4 represent that TNTs could be successfully synthesized. Images received from this section confirm that the structure and morphology of the nanotubes remained largely intact. It was observed that these TNTs have the different length ranging around 50–200 nm. Also, it was observed that these nanotubes have 10–20 nm diameters. Images with high magnification by TEM represent that the inner and outer diameter of these nanotubes is around 2–4.5 nm and 10–20 nm, respectively.

3.2. BET analysis

The contact surface area, the mean value of the pore size, and the pore volume of the synthesized TNT were determined using the BET method. The surface area of the sample was calculated to be 194.4 m^2/g. As the adsorption rate depends on the surface area and the increase in surface area increases the adsorption, it is expected that the adsorption rate will increase dramatically and significantly due to the large difference in surface area of the TNTs and the TiO_2. Figs. 5 and 6 are type IV adsorbing and disposing of isotherms of TNTs. The hysteresis ring in this isotherm is in accordance with the classification of Brunauer–Deming–Deming–Teller, type 3H, which indicates the presence of cavities of mesosize 2–50 nm. Fig. 5 shows the size distribution of the cavities. The size of the cavities of the nanotubes has a wide distribution ranging from 1.5 to 100 nm. The morphology of the nanotubes in Fig. 4 shows that the diameters smaller than 10 nm refer to the cavities inside the nanotubes, or, in other words, the inner diameter of the nanotubes. The cavities larger than 10 nm are related to the grinding of the nanotubes. Synthesis of TNT shows a significant increase in the specific surface area from 10 to 194.386 m^2/g, which is approximately 20-fold higher than titanate material. Table 1 shows surface area, pore volume, and average pore size of synthesized TNT properties.

3.3. Cytotoxicity effect of TNT

For investigation of the cytotoxicity effect of TNT, different dose ranging from 0.1 up to 10 mg/mL was used for MTT assay. Data received from MTT assay represented that the TNT on HUGU cells with 0.01, 0.02, 0.04, 0.08, 0.1, 0.2, 0.4, and 0.5 mg/mL concentrations, had 99.6%, 95.2%, 93.1%, 91.5%, 89.1%, 84.0%, 80.1%, 78.75%, 75.8%, and 73.6% viability, respectively (Fig. 7). These results are in agreement

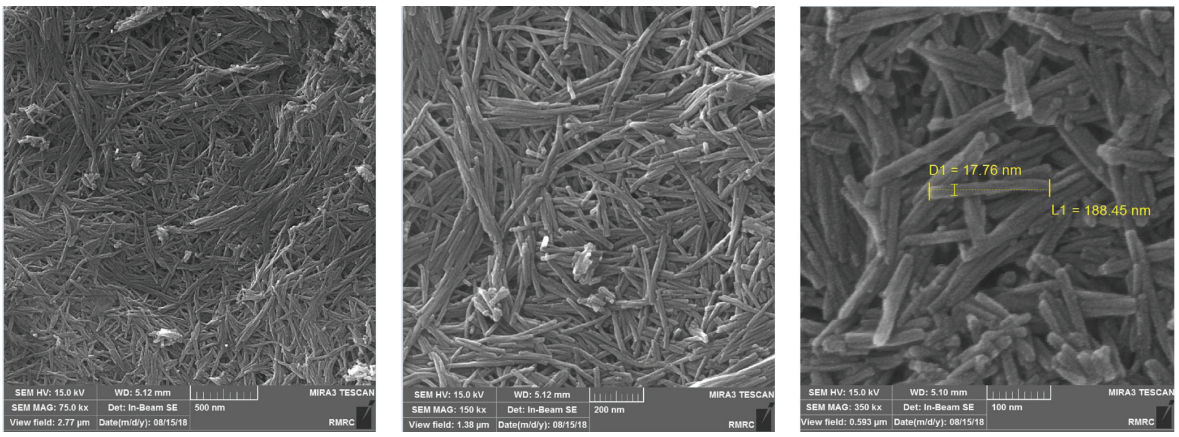

Fig. 3. FESEM images derived from synthetized titanate nanotube.

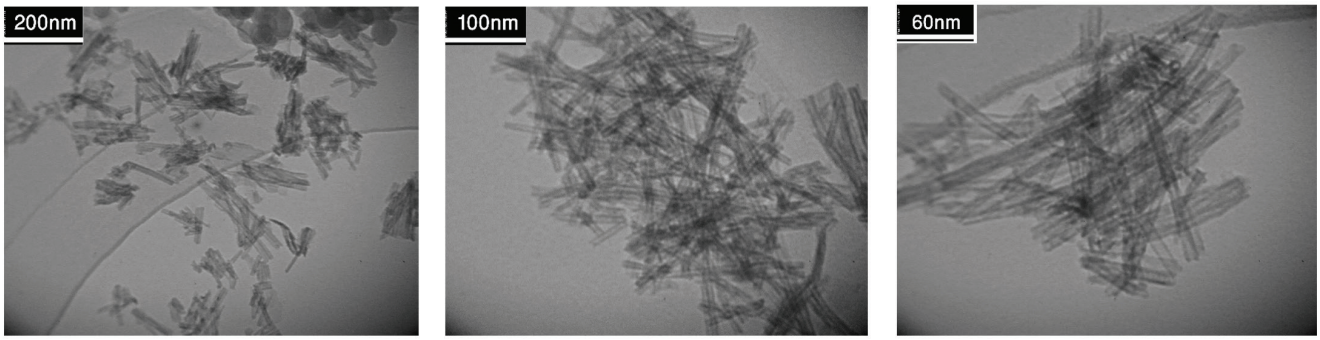

Fig. 4. TEM images derived from synthetized titanate nanotube.

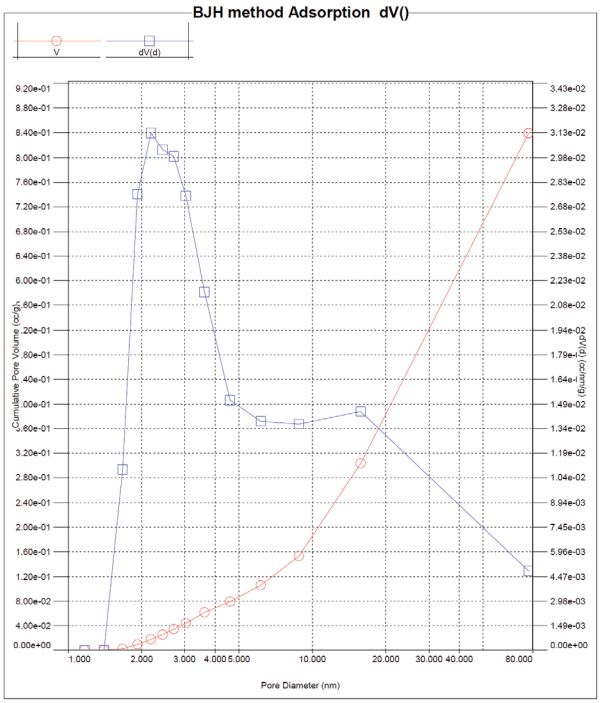

Fig. 5. Distribution of titanate nanotube pore size at 150°C.

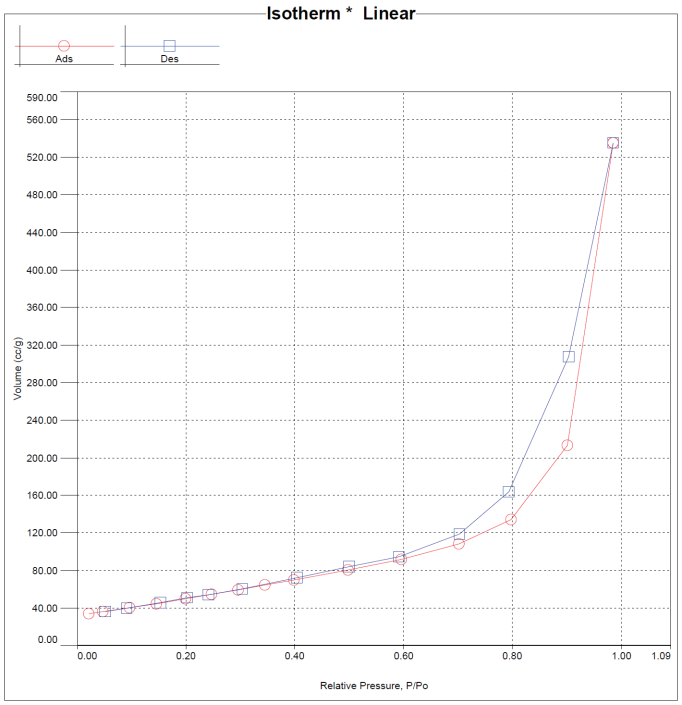

Fig. 6. Adsorption–desorption isotherm of titanate nanotube.

Table 1
Special surface area, pore volume, and pore average size of synthesized titanate nanotube

Pore size (nm)		Pore volume (cm^3/g)		Special surface area (m^2/g)
BJH	BJH	BJH	BJH	BET
Desorption	Adsorption	Desorption	Adsorption	
8.724	2.182	17.09	83.76	194.4

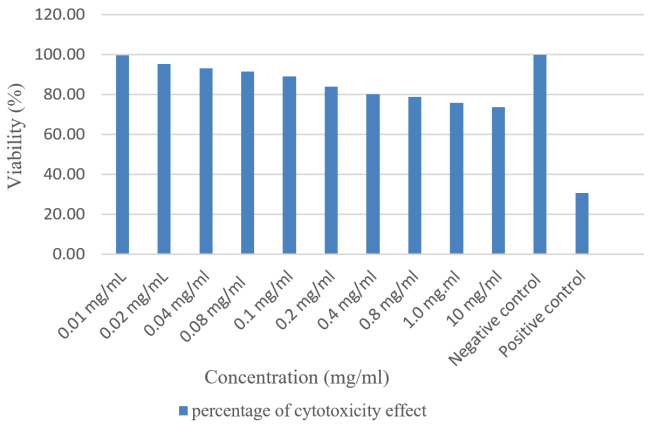

Fig. 7. Cytotoxicity effect of titanate nanotube. HUGU cells were treated with titanate nanotubes in different concentrations for 24 h, and their viability was examined by MTT assay. Untreated control (negative control) was considered as 100% viability, and data are expressed as the percentage of untreated control. Cells treated with 10% DMSO are used as positive control. Data are means of three independent repeats for each experiment.

with the data received from Fenyvesi et al. [26] and Koeneman et al. [29] which analyzed $CaCO_2$ cell viability when exposed to the different dose of TNT.

3.4. Investigation of different variables for tTNT adsorption rate

This study showed that the pH strongly influences the ion adsorption rate. The results in Fig. 8(a) demonstrate that the increase of pH up to 6 leads to increase in the amount of adsorption of cesium ion. At pH below 3, the acidic condition leads to the replacement of the H^+ ion with Na^+ which reduced the adsorption capacity of cesium. In addition, at pH 6, the adsorption rate decreases due to the presence of OH– functional group in the NaOH solution and leads to the precipitation of cesium salts. These results are in accordance with Dongjiang et al. [27] reports.

To obtain optimal adsorbent content, 0.01–0.25 g per 25 mL of nanotube titanate adsorbent were utilized. It was shown that by increasing the amount of adsorbent, the adsorption rate would also increase as the adsorbent contact surface increases. This is because, as a number of adsorbent increases, the possibility of contacting particles with adsorbents also increases and much more ions can establish on the surface of

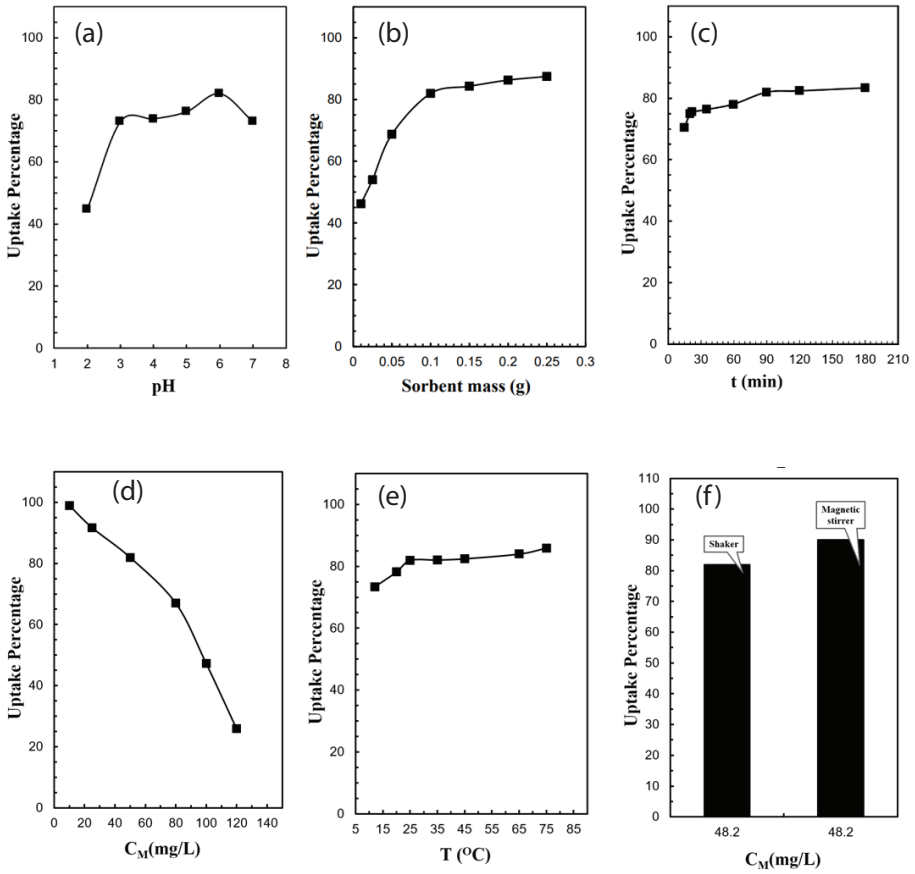

Fig. 8. Effect of the pH (a), sorbent mass (b), time (c), cesium mass (d), temperature (e), and stirrer type (f) on the cesium uptake.

the adsorbents. As shown in Fig. 8(b), the adsorption of cesium ions has increased with increasing the amount of adsorbent.

Moreover, the data received from AAS analysis showed the adsorption rate of radioactive cesium by TNTs in the experimental conditions of pH = 6 and cesium concentration of 50 mg/L, after 10, 20, 35, 60, 120, and 180 min. The uptake percentages were 70.5, 75.0, 80.4, 81.2, 82.4, and 83.3, respectively (Fig. 8(b)). This result confirms that elevating the time can increase the adoption rate in a gentle slope.

As shown in Fig. 8(c), in the first 10 min of the adsorption process, the adsorption rate is extremely high; and then the rate of adsorption decreased. The mechanism of adsorption of exchanged ions on the adsorbent can be explained by the way that the ions first adsorbed at high speed on the surface exchange locations (incorporated in the TNT surface) and after the saturation of these sites, these ions entered into the internal cavities, which are referred to as the internal influence of particles (between the TiO_6 layers).

Due to the fact that a distinct number of exchangeable positions are active and a certain amount of exchangeable ions exist in each unit of ion exchange, by creating a balance between two phases and the passage of time, these sites are saturated and adsorption reach to the maximum rate, but the rate of adsorption is constant.

The inhomogeneity of adsorption sites may be a reason for the multi-rate adsorption characteristics to occur. Different access to surface porosity and multiple adsorption sites with different adsorption powers leads to heterogeneity of the surface and the difference in the rate of adsorption.

The influence of cesium ion concentrations on the ion exchange capability of TNT was investigated subsequently. It is observed in Fig. 8(d) that due to the increase in the concentration of cesium ions in the solution, the adsorption rate decreased. Finally, a solution containing 10 mg/L of cesium ion represented 100% absorption rate and a solution containing 120 mg/L of cesium just could be adsorbed only 25% of the substance. This phenomenon can be described in such a way that by increasing the cesium concentration, the rate of available sites for absorption on the surface of the TNT adsorbent is less, so the percentage of metal ion adsorption decreases.

To study the effect of temperature on adsorption rate, 25 mL of cesium ions at a concentration of 50 mg/L were performed at 10°C–75°C. As shown in Fig. 8(e), the rate of absorption increases with increasing temperature from 10°C to 25°C, but then it showed an irregular pattern by decreasing (at 25°C–50°C) and then increasing (at 50°C–75°C) the temperature. It is probable that both the chemical and physical adsorption mechanisms are simultaneously in competition with each other. Therefore, at the first stage of interaction (10°C–25°C), chemical interactions are predominant and the reaction is heat releasing. In addition, in the

next stage, (25°C–50°C) physical interactions predominate, and the reaction is heat catching.

The results of agitator type (magnetic stirrer or mechanical shaker) experiments (Fig. 8(f)) showed that the use of a magnetic stirrer would cause a condition which cesium ions could be adsorbed with much more efficiency using TNT.

Furthermore, since thermostatic stirrer carries out the operation, it is likely that magnetic stirrer would provide better conditions for contacting between the two solid phases of the nanotube and a solution containing cesium ion [35]. Thus, the absorption rate would be at the highest level.

To summarize an optimum condition, 0.1 g of TNT was exposed to 50 mg/L of cesium ion at pH = 6 and 25°C temperature in 25 mL of wastewater. The entire solution was exposed to a magnetic stirrer at a rate of 150 rpm. The experimental analysis confirmed that after 90 min, around 85% of cesium ion (42.5 mg/L) could be absorbed in high efficiency.

3.5. Isotherms

Modeling of isotherm data can cause a relevance and proximity between the predictions and experimental data. The adsorption isotherms are mathematical models that represent the distribution of the adsorbed substance among the solution and the adsorbent; which is based on a set of assumptions including the heterogeneity/homogeneity of adsorbents, the type of exposure, and the possibility of interaction between the adsorbed substance [36]. In this investigation, Langmuir and Freundlich isotherm models were used to analyze the equilibrium information. The isotherm is useable for monolayer adsorption onto a surface containing a finite number of identical sites. The form of the Langmuir isotherm can be described by Eq. (2) [37]:

$$\frac{C_e}{q_e} = \frac{C_e}{Q^\circ} + \frac{1}{Q^\circ b} \tag{2}$$

where C_e and q_e are the concentration of metal ions remaining in the solution during equilibrium (mg/L) and adsorbed after equilibrium (mg/g), respectively. Q° is the maximum sorption capacity, which is described based on the amount of adsorbed substance at complete monolayer coverage (mg/g), and b is considered as a constant which is related to the temperature of adsorption (L/mg).

The Freundlich isotherm model specifies that the ratio of the amount of solute adsorbed to the amount of solute concentration is a function of that solution. This model can apply for several kinds of sorption sites on the solid, which appropriately represents the sorption data at low and intermediate concentrations on heterogeneous surfaces. The model is described in Eq. (3) [38]:

$$\log q_e = \log K_F + \frac{1}{n}\log C_e \tag{3}$$

where K_F is the constant, which is revealing the relative ion exchange capacity of the adsorbent, and $1/n$ is the constant, which is indicating the intensity of the ion exchange/adsorption.

The parameters, which are calculated from the Freundlich and Langmuir models for cesium ion, are summarized in Table 2. According to Table 2, the higher correlation coefficients for the Freundlich model indicate that this model can describe the adsorption data better than the Langmuir one. The obtained $1/n$ ($0 < 1/n < 1$) corresponds to a heterogeneous surface with a descriptive distribution of the energy corresponding to the adsorption sites.

3.6. Investigation of the thermodynamic parameters

Thermodynamic parameters were analyzed during the adsorption process using Eq. (4) [39]:

$$\ln K_d = \frac{-\Delta H^\circ}{RT} + \frac{\Delta S^\circ}{R} \tag{4}$$

where ΔH°, ΔS°, T, and R are the standard enthalpy, standard entropy, the temperature in Kelvin, and the gas constant, respectively. The evaluation of enthalpy and entropy can be acquired from the linear variation of $\ln K_d$ with bilateral temperature (Fig. 9).

Meanwhile, the standard Gibbs free energy (ΔG°) for cesium adsorption was calculated from the following well-known equation (Eq. (5)):

Table 2
Parameters of Langmuir and Freundlich isotherms at 298 K

Ion	Langmuir constants			Freundlich constants		
	Q° (mg/g)	b (L/mg)	R^2	K_f (mg/g)	n	R^2
Cesium	30.581	0.082	0.917	3.516	1.875	0.981

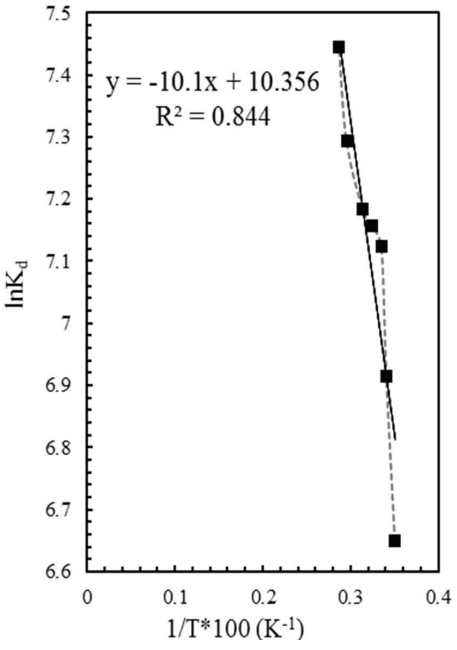

Fig. 9. Influence of the temperature on uptake of the cesium.

Table 3
Thermodynamic parameters for cesium adsorption onto nanotube titanate

Cesium ion	Temperature (K)	$-\Delta G°$ (kJ/mol)	$\Delta H°$ (kJ/mol)	$\Delta S°$ (kJ/K mol)
	285	24.401		
	293	25.089		
	298	25.518	0.080	0.086
	305	26.119		
	318	27.236		
	338	28.954		
	348	29.813		

Table 4
Kinetic parameters for the adsorption of cesium adsorption onto nanotube titanate

Ion	Kinetic models	Parameters	
Cesium	First order $\log(q_t - q_e) = \log q_e - \frac{K_1}{2.303}t$	K_2	0.009
		R^2	0.773
	Pseudo-second-order $\frac{t}{q_t} = \frac{1}{K_2 q_e^2} + \frac{1}{q_e}t$	K_2	–0.093
		R^2	1.000

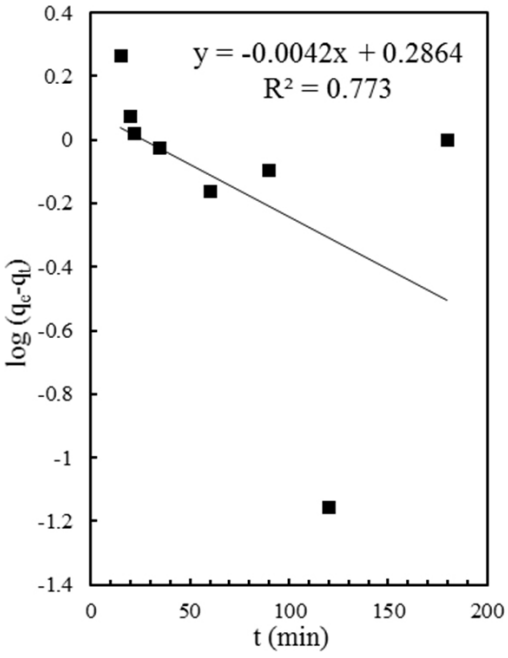

Fig. 10. First order kinetic plot of cesium adsorption on nanotube titanate.

$$\Delta G° = \Delta H° - T\Delta S° \quad (5)$$

The amount of $\Delta H°$, $\Delta S°$, and $\Delta G°$ are included in Table 3. These results represent that the value of $\Delta H°$ is positive and the final value of $\Delta G°$ is negative for cesium ion adsorption; which shows that the cesium ion adsorption is an endothermic and a spontaneous process in the presence of synthesized TNT adsorbent.

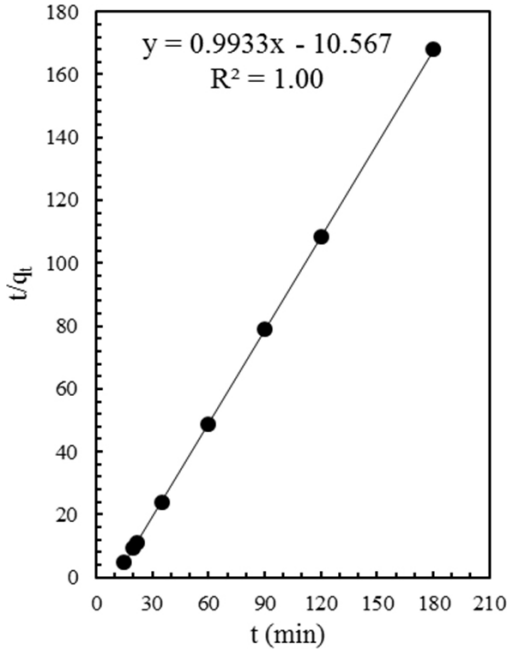

Fig. 11. Pseudo-second-order kinetic plot of cesium adsorption on nanotube titanate.

3.7. Kinetic analysis

The adsorption rate of cesium ion by TNT was calculated by equilibrating 0.1 g TNT adsorbent with a series of cesium ion solutions for different time intervals. Fig. 8(c) shows the amount of cesium adsorption in a distinct period of time (min). The results have demonstrated that ~70% of the adsorbed cesium take place at a time duration less than 30 min, and the time required for cesium ion to reach equilibrium is around 90 min.

For investigation of the specific rate constant of the cesium adsorption, the kinetic data have been analyzed by the reversible first order and pseudo-second-order kinetic model. The mathematical linear equation and the plots for analyzing the data have been presented in Table 4.

Figs. 10 and 11 demonstrate the reversible first order and pseudo-second-order kinetic model diagrams for cesium adsorption, respectively. The associated kinetic parameters have been evacuated and the only best-fit plot is shown in Table 4. The results received from the analysis of the present data represented that cesium adsorption on nanotube titanate has been best described by a pseudo-second-order kinetic equation (R^2 = 1.000).

4. Conclusion

In this study, TNTs can be fabricated by hydrothermal method at low cost, in order to remove cesium ion discarded to the aqueous environment. The results obtained from the XRD and BET analysis represented a nanoscale structure with

anatase phase which has a specific surface area of 194.4 m^2/g. AAS and kinetic analysis on TNT sample further determined the optimized experimental condition for cesium adsorption using TNT. Utilization of 300°C as calcination temperature maintains a highly stable tubular morphology of nanotubes in anatase phase. Furthermore, cesium adsorption using the prepared TNT represented an endothermic and a spontaneous process. Moreover, based on the data received from MTT assay it was shown that TNT can be considered as a safe adsorbent, which can be widely used for the removal of aquatic pollutant.

Acknowledgments

Nuclear Science and Technology Research Institute supported this research. The authors would like to thank their colleagues from the institute who provided expertise and comments that greatly assisted the research. The authors would also like to express their gratitude to the colleagues from East Tehran Branch of Islamic Azad University for sharing their experience during the project. The authors are also immensely grateful to Dr. Zahra Elyasi Gorji for her comments and review on an earlier version of the manuscript, although any errors are our own and should not tarnish the reputations of these esteemed persons.

Conflict of interest

The authors declare that they have no conflict of interest.

References

[1] A.N. Jha, Genotoxicological studies in aquatic organisms: an overview, Mutat. Res. Fund. Mol., 552 (2004) 1–17.
[2] Y. Zhang, Z. Jiang, J. Huang, L.Y. Lim, W. Li, J. Deng, D. Gong, Y. Tang, Y. Lai, Z. Chen, Titanate and titania nanostructured materials for environmental and energy applications: a review, RSC Adv., 5 (2015) 79479–79510.
[3] M.R. Awual, T. Yaita, Y. Miyazaki, D. Matsumura, H. Shiwaku, T. Taguchi, A reliable hybrid adsorbent for efficient radioactive cesium accumulation from contaminated wastewater, Sci. Rep., 6 (2016) 19937.
[4] C. Delchet, A. Tokarev, X. Dumail, G. Toquer, Y. Barre, Y. Guari, C. Guerin, J. Larionova, A. Grandjean, Extraction of radioactive cesium using innovative functionalized porous materials, RSC Adv., 2 (2012) 5707–5716.
[5] B. Filipowicz, M. Pruszyński, S. Krajewski, A. Bilewicz, Adsorption of ^{137}Cs on titanate nanostructures, J. Radioanal. Nucl. Chem., 301 (2014) 889–895.
[6] D. Yang, S. Sarina, H. Zhu, H. Liu, Z. Zheng, M. Xie, S.V. Smith, S. Komarneni, Capture of radioactive cesium and iodide ions from water by using titanate nanofibers and nanotubes, Angewandte Chemie Int. Ed., 50 (2011) 10594–10598.
[7] K. Haselwandter, M. Berreck, P. Brunner, Fungi as bioindicators of radiocaesium contamination: Pre- and post-Chernobyl activities, Trans. British Mycol. Soc., 90 (1988) 171–174.
[8] T. Sawidis, G. Heinrich, M.K. Chettri, Cesium-137 monitoring using mosses from Macedonia, N. Greece, Water Air Soil Pollut., 110 (1999) 171–179.
[9] S. Chibowski, M. Reszka, Investigation of Lublin town environment contamination by radionuclides and heavy metals with application of *Parmeliaceae lichens*, J. Radioanal. Nucl. Chem., 247 (2001) 443–446.
[10] A. Dolhanczuk-Srodka, M. Waclawek, Cesium-137 translocation in environment, Ecol. Chem. Eng. Sci., 14 (2007) 147–168.
[11] J.E. Martin, F.D. Fenner, Radioactivity in municipal sewage and sludge, Public Health Rep., 112 (1997) 308.
[12] S. Sarina, A. Bo, D. Liu, H. Liu, D. Yang, C. Zhou, N. Maes, S. Komarneni, H. Zhu, Separate or simultaneous removal of radioactive cations and anions from water by layered sodium vanadate-based sorbents, Chem. Mater., 26 (2014) 4788–4795.
[13] K. Shakir, M. Sohsah, M. Soliman, Removal of cesium from aqueous solutions and radioactive waste simulants by coprecipitate flotation, Sep. Purif. Technol., 54 (2007) 373–381.
[14] V. Kouřím, Coprecipitation of carrier-free caesium with 12-heteropolyacids in a strong acid medium, J. Inorg. Nucl. Chem., 12 (1960) 370–372.
[15] E. Makrlík, P. Toman, P. Vaňura, B.A. Moyer, Interaction of the cesium cation with calix [4] arene-bis (t-octylbenzo-18-crown-6): extraction and DFT study, J. Mol. Struct., 1033 (2013) 14–18.
[16] E. Makrlik, P. Vaňura, Synergistic extraction of some univalent cations into nitrobenzene by using cesium dicarbollylcobaltate and dibenzo-30-crown-10, J. Radioanal. Nucl. Chem., 295 (2013) 911–914.
[17] A.L. Mascarelli, Funding Cut for US Nuclear Waste Dump, Nature Publishing Group, 2009.
[18] S. Tsuruoka, B. Fugetsu, F. Khoerunnisa, D. Minami, K. Takeuchi, M. Fujishige, T. Hayashi, Y.A. Kim, K.C. Park, M. Asai, Intensive synergetic Cs adsorbent incorporated with polymer spongiform for scalable purification without post filtration, Mater. Express., 3 (2013) 21–29.
[19] N. Ding, M.G. Kanatzidis, Selective incarceration of caesium ions by Venus flytrap action of a flexible framework sulfide, Nat. Chem., 2 (2010) 187–191.
[20] L. Van Loon, B. Baeyens, M. Bradbury, The sorption behaviour of caesium on Opalinus clay: a comparison between intact and crushed material, Appl. Geochem., 24 (2009) 999–1004.
[21] Á. Kukovecz, K. Kordás, J. Kiss, Z. Kónya, Atomic scale characterization and surface chemistry of metal modified titanate nanotubes and nanowires, Surf. Sci. Rep., 71 (2016) 473–546.
[22] H.Y. Zhu, Y. Lan, X. Gao, S.P. Ringer, Z. Zheng, D.Y. Song, J.-C. Zhao, Phase transition between nanostructures of titanate and titanium dioxides via simple wet-chemical reactions, J. Am. Chem. Soc., 127 (2005) 6730–6736.
[23] Y.I. Kim, S. Salim, M.J. Huq, T.E. Mallouk, Visible-light photolysis of hydrogen iodide using sensitized layered semiconductor particles, J. Am. Chem. Soc., 113 (1991) 9561–9563.
[24] N. Sukpirom, M.M. Lerner, Preparation of organic–inorganic nanocomposites with a layered titanate, Chem. Mater., 13 (2001) 2179–2185.
[25] D.J. Yang, Z.F. Zheng, H.Y. Zhu, H.W. Liu, X.P. Gao, Titanate nanofibers as intelligent absorbents for the removal of radioactive ions from water, Adv. Mater., 20 (2008) 2777–2781.
[26] F. Fenyvesi, Z. Kónya, Z. Rázga, M. Vecsernyés, P. Kása, K. Pintye-Hódi, I. Bácskay, Investigation of the cytotoxic effects of titanate nanotubes on $CaCO_2$ cells, AAPS PharmSciTech, 15 (2014) 858–861.
[27] Y. Dongjiang, S. Sarina, Z. Huaiyong, L. Hongwei, Z. Zhanfeng, X. Mengxia, S.V. Smith, K. Sridhar, Capture of radioactive cesium and iodide ions from water by using titanate nanofibers and nanotubes, Angewandte Chemie Int. Ed., 50 (2011) 10594–10598.
[28] N. Liu, X. Chen, J. Zhang, J. Schwank, A review on TiO_2-based nanotubes synthesized via hydrothermal method: formation mechanism, structure modification, and photocatalytic applications, Catal. Today, 225 (2014) 34–51.
[29] B.A. Koeneman, Y. Zhang, P. Westerhoff, Y. Chen, J.C. Crittenden, D.G. Capco, Toxicity and cellular responses of intestinal cells exposed to titanium dioxide, Cell Biol. Toxicol., 26 (2010) 225–238.
[30] J. Zhang, W. Song, J. Guo, J. Zhang, Z. Sun, L. Li, F. Ding, M. Gao, Cytotoxicity of different sized TiO_2 nanoparticles in mouse macrophages, Toxicol. Ind. Health, 29 (2013) 523–533.
[31] T. Mosmann, Rapid colorimetric assay for cellular growth and survival: application to proliferation and cytotoxicity assays, J. Immunol. Methods, 65 (1983) 55–63.

[32] C.-C. Tsai, H. Teng, Structural features of nanotubes synthesized from NaOH treatment on TiO_2 with different post-treatments, Chem. Mater., 18 (2006) 367–373.
[33] M. Zhang, Z. Jin, J. Zhang, X. Guo, J. Yang, W. Li, X. Wang, Z. Zhang, Effect of annealing temperature on morphology, structure and photocatalytic behavior of nanotubed $H_2Ti_2O_4(OH)_2$, J. Mol. Catal. A, 217 (2004) 203–210.
[34] W. Wang, J. Zhang, H. Huang, Z. Wu, Z. Zhang, Investigation of monolayer dispersion of benzoic acid supported on the surface of H-titanate nanotubes, Appl. Surf. Sci., 253 (2007) 5393–5399.
[35] Operational Control of Coagulation and Filtration Processes, American Water Works Association, 2011.
[36] A. Nilchi, T.S. Dehaghan, S.R. Garmarodi, Kinetics, isotherm and thermodynamics for uranium and thorium ions adsorption from aqueous solutions by crystalline tin oxide nanoparticles, Desalination, 321 (2013) 67–71.
[37] I. Langmuir, The adsorption of gases on plane surfaces of glass, mica and platinum, J. Am. Chem. Soc., 40 (1918) 1361–1403.
[38] H. Freundlich, Über die Adsorption in Lösungen, in Zeitschrift für Physikalische Chemie, 1907, p. 385.
[39] K. Banerjee, G.L. Amy, M. Prevost, S. Nour, M. Jekel, P.M. Gallagher, C.D. Blumenschein, Kinetic and thermodynamic aspects of adsorption of arsenic onto granular ferric hydroxide (GFH), Water Res., 42 (2008) 3371–3378.